Splitting f_{max}: separating site-controlled and source-controlled contributions into the upper cutoff of acceleration spectrum of a local earthquake

A.A Gusev [1,2], ***E.M.Guseva*** [2]

Petropavlovsk-Kamchatsky, RUSSIA

[1]Institute of Volcanology and Seismology, FED, Russian Ac. Sci.

[2] Kamchatka Branch, Geophysical Service, Russian Ac. Sci.

Starting point: "ω^{-2}" or "omega-square" model

for the shape of far-field earthquake source spectrum

***Single corner** Aki 1967, Brune 1970*

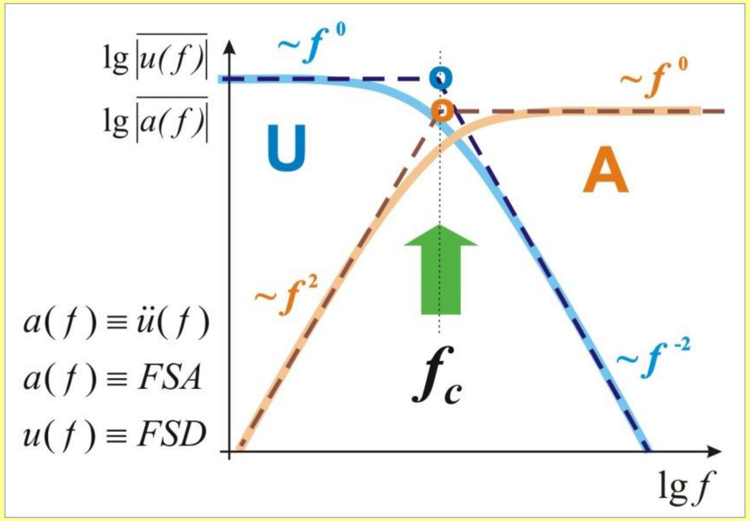

Single-corner displacement *u*(*f*) spectrum after Aki(1967), also the simpler, standard variant after (Brune 1970); ε=1
single corner frequency f_c

***Double corner,** Brune 1970 : ε<1*

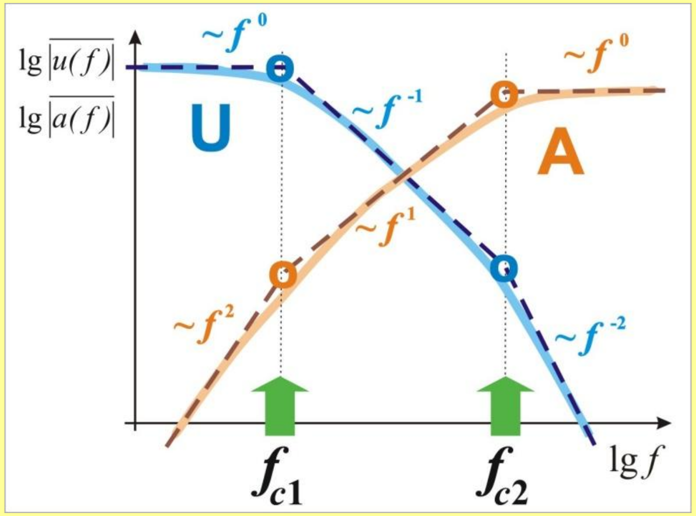

Two-corner *u*(*f*) spectrum, advanced, non-standard variant after (Brune 1970) ; ε<1
two corner frequencies f_{c1}, f_{c2}

Key points:

1. ***flat (f^0) source acceleration spectrum***
2. ***f_{c2} is commonly seen in observed spectra***

“Source-controlled f_{max}”, or 3rd corner frequency, f_{c3} : does it exist? how it scales?

HISTORY

Hanks (1982) emphasized the “f_{max}” phenomenon: $a(f)$ shows **HF cutoff**.

Papageorgiou and Aki(1983) and *Gusev* (1983) ascribed it to **source**; *Aki* (1988) noticed f_{max} vs M_0 trend with **unusual scaling** that might support this idea

Hough and Anderson (1984) have shown convincingly that **site-related loss** controls f_{max}

Still, accumulated evidence suggests that f_{max} is a complex feature; it incorporates **both site**-controlled and **source**-controlled components

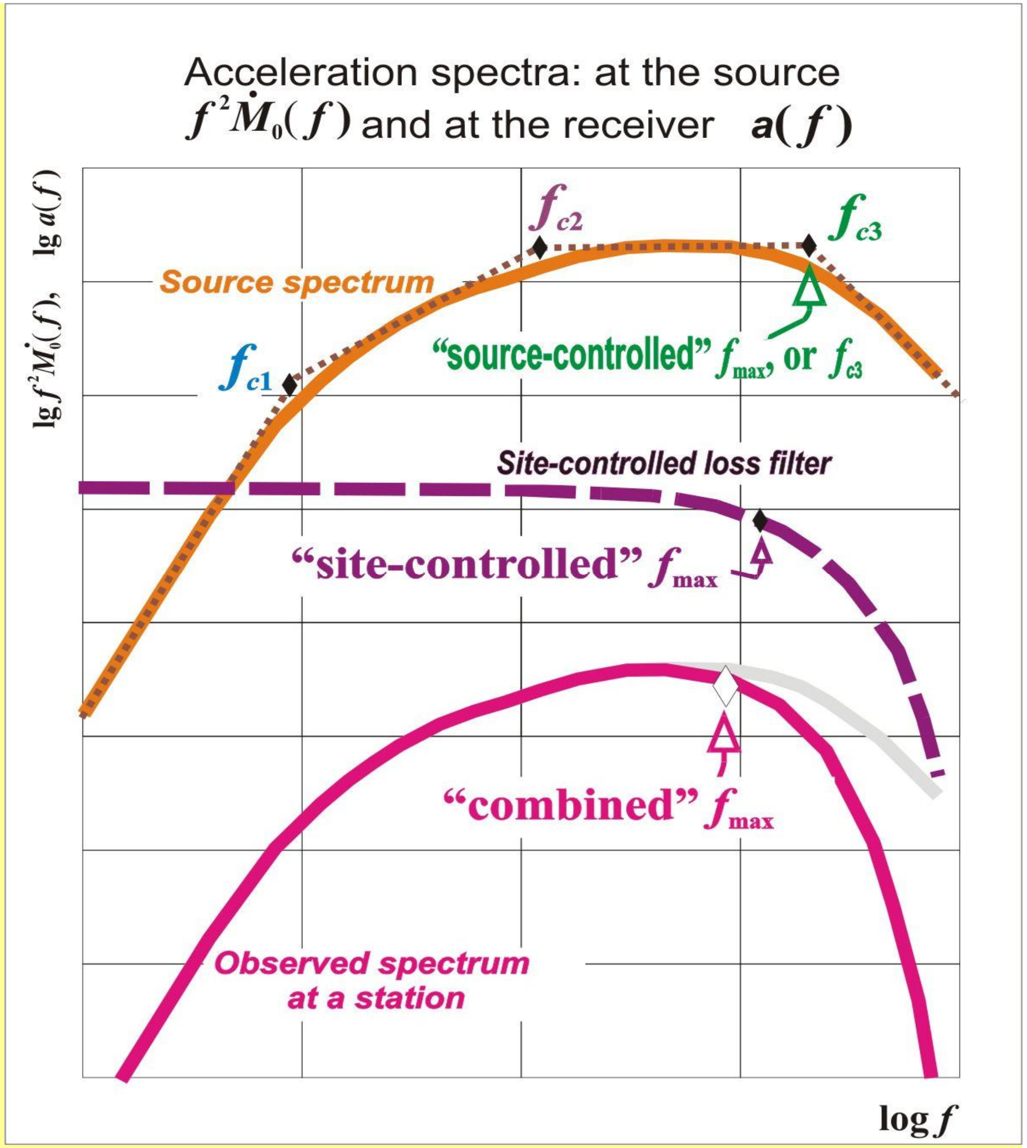

Outline of the study

1. Compile a preliminary attenuation model ($Q(f), \kappa_0$)
2. (a) Use it to correct observed spectra for propagation loss
   (b) From corrected spectra, extract f_{c3} and also f_{c2}
3. Using the observed spectra within the limited [f_{c2} ,f_{c3}] frequency range, adjust the attenuation model
4. Repeat steps 2 an 3 until convergence
5. Discuss the obtained f_{c3} data set

Data set used

Records of ***S-wave*** group
by low-gain digital accelerograph
(HN channel, ***80 sps***)
of IRIS BB station PET

439 records of 1993-2005
+ additional ***130***

Hypo distance ***80-220 km***

Depth range ***0-200 km***,
mostly 0-50 km

M_L = ***4 - 6.5***

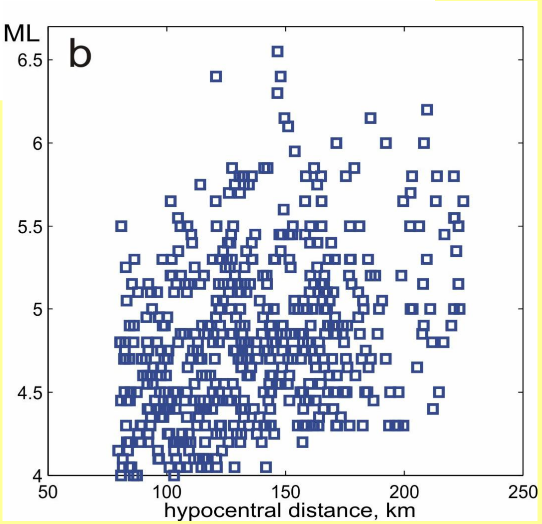

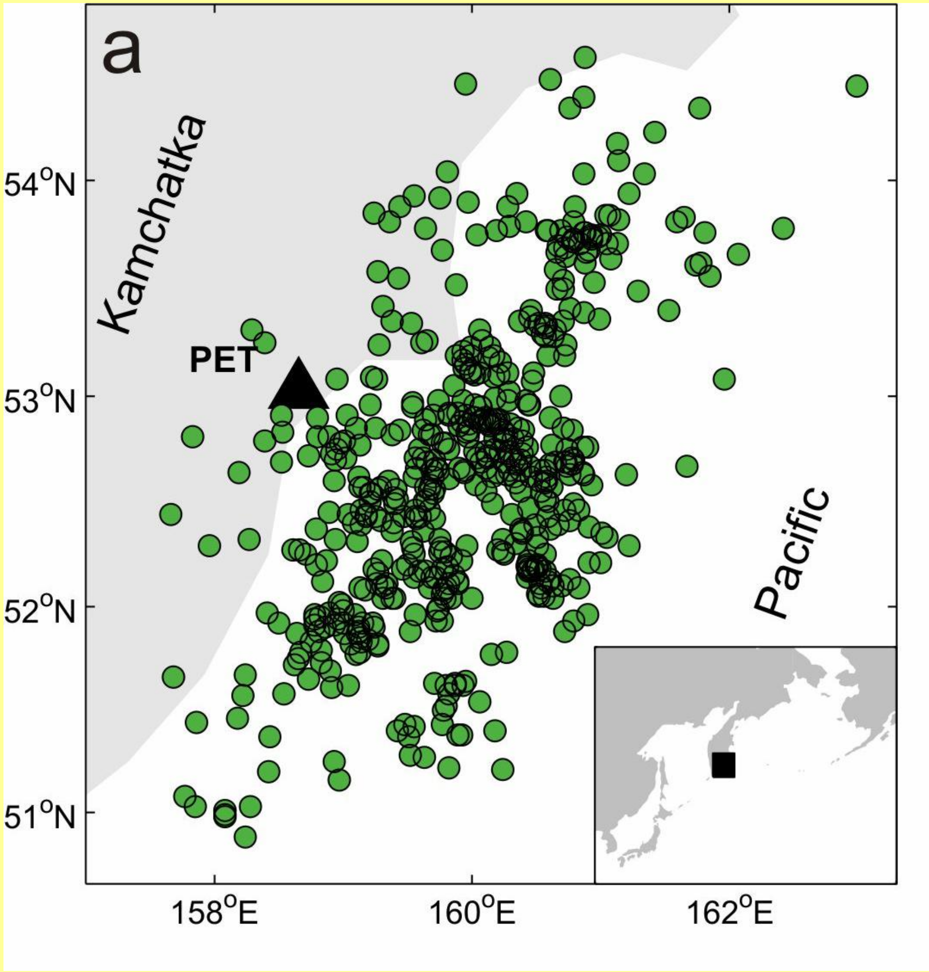

Compilation of the initial loss model on the basis of earlier results

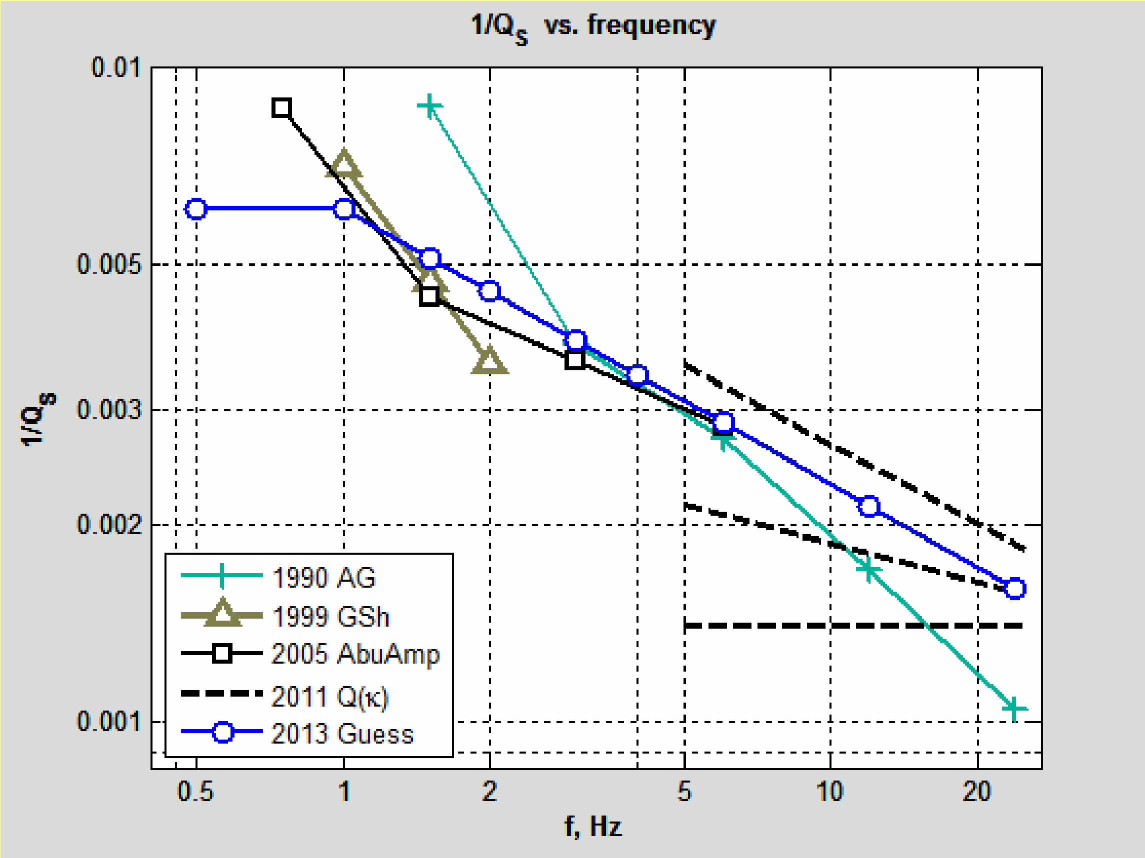

accepted $\mathbf{Q_S(f)}$ model:

Main sources used in compilation:

in the 1-6 Hz band from (Abubakirov 2005) who used coda-normalized spectral levels of band-filtered data

in the 5-25 Hz band based on (Gusev Guseva 2011) who analyzed kappa values;

accepted trend at r=100 km:

$\boldsymbol{Q_S(f)=165\, f^{0.42}}$

also $\boldsymbol{\kappa_0=0.016}$ **s**

and slow decay of $\boldsymbol{Q_S^{-1}}$ vs. $\boldsymbol{r}$

Example of processing in a case when each of f_{c1} , f_{c2} and f_{c3} is observable

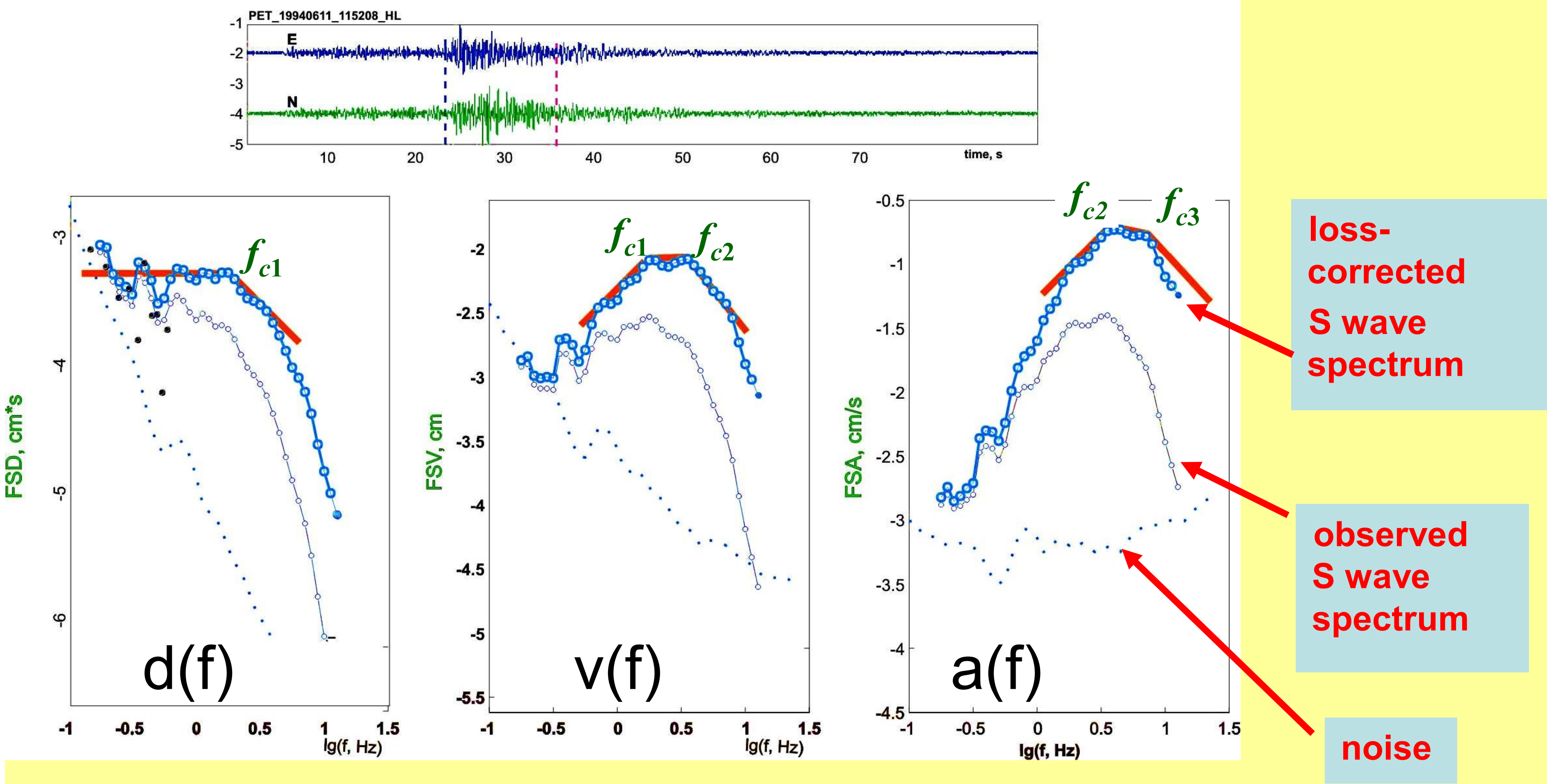

spectral smoothing window used:
0.15 log units (1/2 octave)

when picking f_{ci}, slope of selected "plateaus"
in v(f) and a(f) plots was kept in the range ±0.5

More example cases: f_{c3} may be observable or unobservable/absent

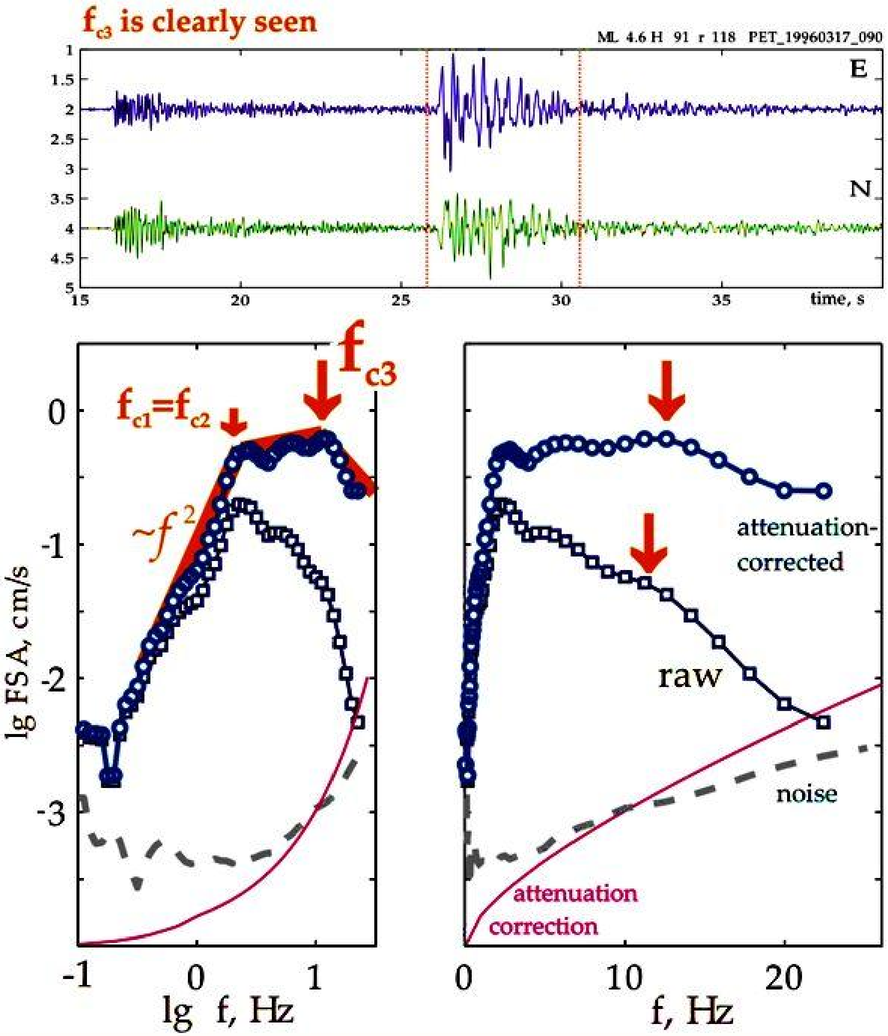

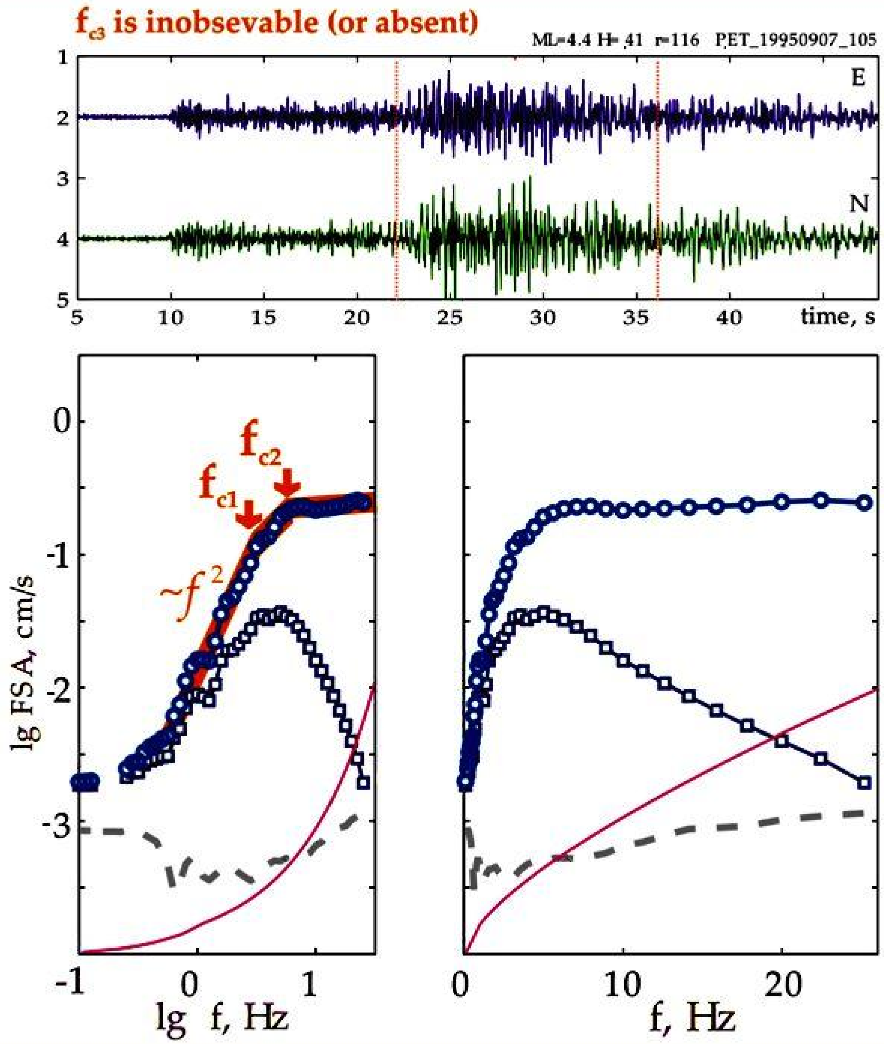

Here is why f_{c3} is difficult to notice when working in the log-linear scale

Finding new adjusted *S*-wave attenuation model. 1. Setting the model

Assumed attenuation model for loss factor in *S*-wave Fourier spectrum:

$$-\log_e \{A(f) / A_0(f)\} = \pi f \kappa_0 + \pi f(r/c)Q^{-1}(f, r)$$

where

r - hypocentral distance

κ_0 – constant loss factor for a site; $\kappa_0 \approx \ln 2/\pi f_{\text{max-loss}}$

c - wave velocity; and $Q(f,r)$ – path quality factor:

$$Q^{-1}(f, r)=Q_0^{-1} (f/f_0)^{-\gamma} (1+q(r-r_0)/r_0)$$

where f_0 =1 Hz, r_0 =100 km, c=3.8km/c;

and **unknowns in inversion** are: κ_o, Q_o, γ, q

Finding new adjusted *S*-wave attenuation model. 2. Inversion

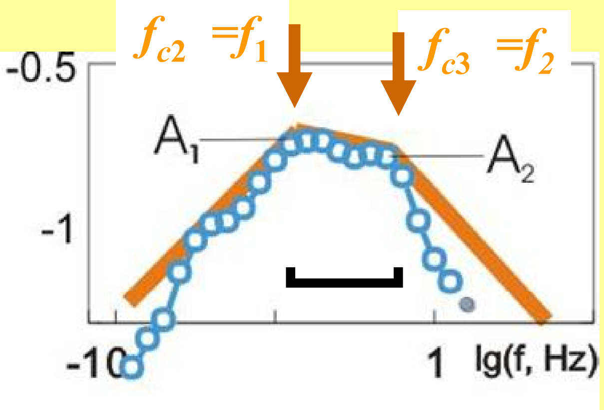

Parameters of observations used in inversion are
spectral amplitudes A_1 and A_2
at the ends of the f_1 - f_2 spectrum segment
(assumed to be flat in the true source spectrum)
the condition of minimum width: $\Delta f = f_1 - f_2 > 2$ Hz
makes a system of N=384 equations; using weight=1/Δf

Denote κ_0 , Q_0^{-1}, γ and q as $x_i = \{x_1, x_2, x_3, x_4\}$; $y_j = \log_e A_2 / A_1$

Obtain the system of N equations

$$y_j = F_j(x_i) + \varepsilon_j$$

where

$$F_j(x_i) = -\pi Q_0^{-1}\left(f_2^{1-\gamma} - f_1^{1-\gamma}\right)\left(1 + q\frac{r_j - 100}{100}\right)\frac{r_j}{c} - \pi\kappa_0\left(f_2 - f_1\right)$$

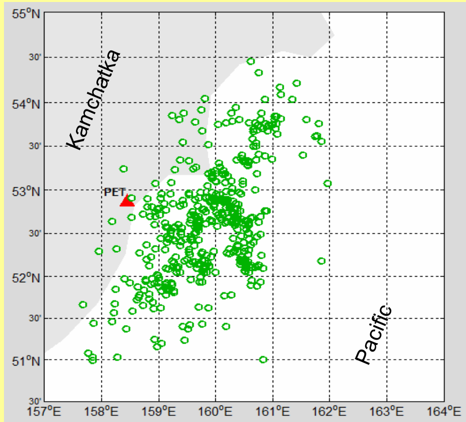

Finding new adjusted *S*-wave attenuation model. 3.Result

Nonlinear inversion procedure:
Nelder-Mead (1964) simplex method

Error bounds: determined using
"delete-d jackknife method"

Inverted 2014 (1st iteration):
$Q_S(f)=(140\pm33)\,f^{\,0.54\pm0.08}$ $\kappa_0=0.027\pm0.07$ s
Inverted 2015 (2nd iteration):
$Q_S(f)=164\,f^{\,0.59}$ $\kappa_0=0.034$

Residuals of $\delta\log A = log(A_2/A_1)$ fitted by the inverted attenuation model:
histogram and plots of $\delta\log A$ against f_{top}, r, *depth*, and M_L

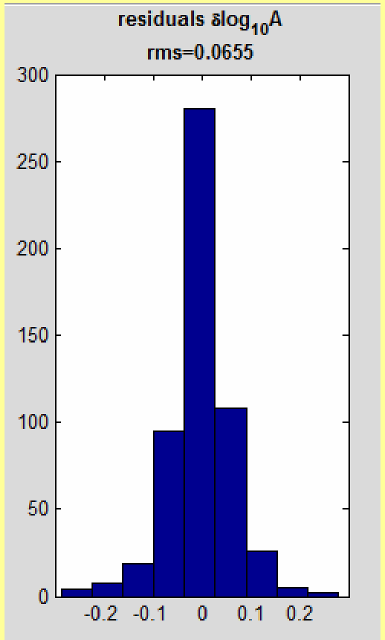

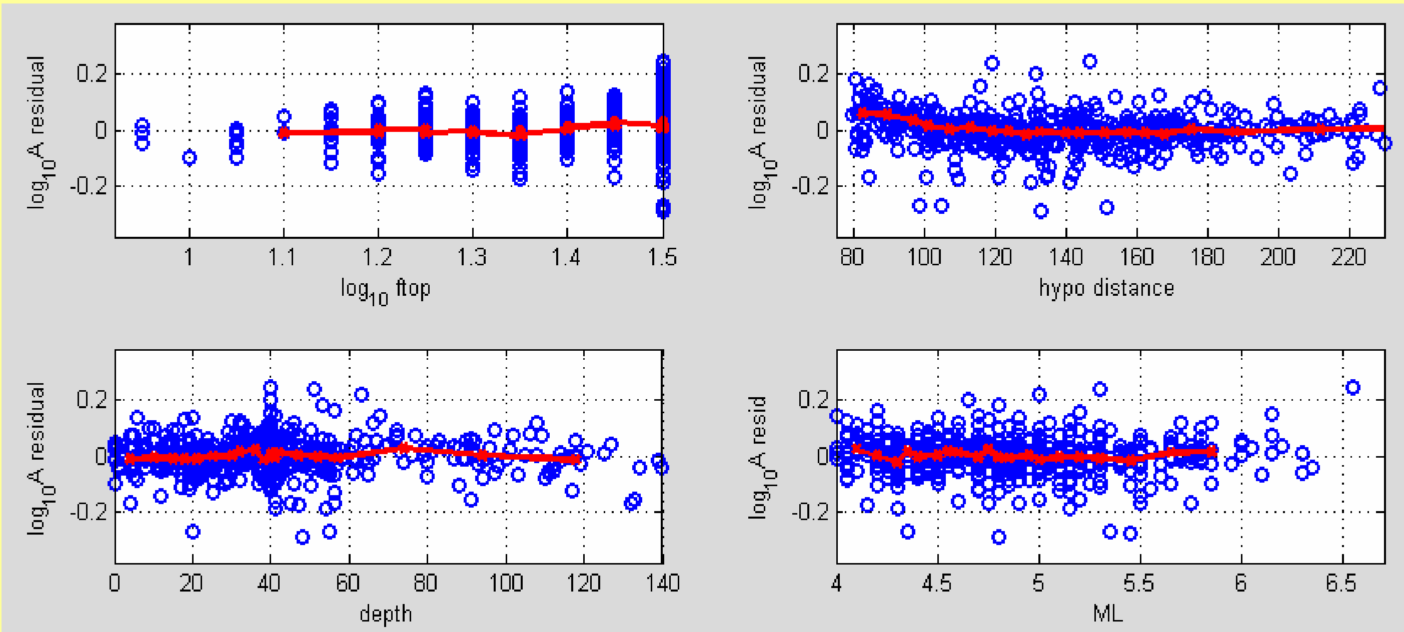

Comparing initial and inverted loss models

$Q_S(f\,|r{=}100\text{km})$:

Guess 2013:

$Q_S(f)=165\,f^{\,0.42}$ + $\kappa_0=0.016$ s

Inverted 2014 (1st iteration):

$Q_S(f)=(140\pm33)\,f^{\,0.54\pm0.08}$ + $\kappa_0=0.027\pm0.07$ s

Inverted 2015 (2nd iteration):

$Q_S(f)=164\,f^{\,0.59}$ + $\kappa_0=0.034$

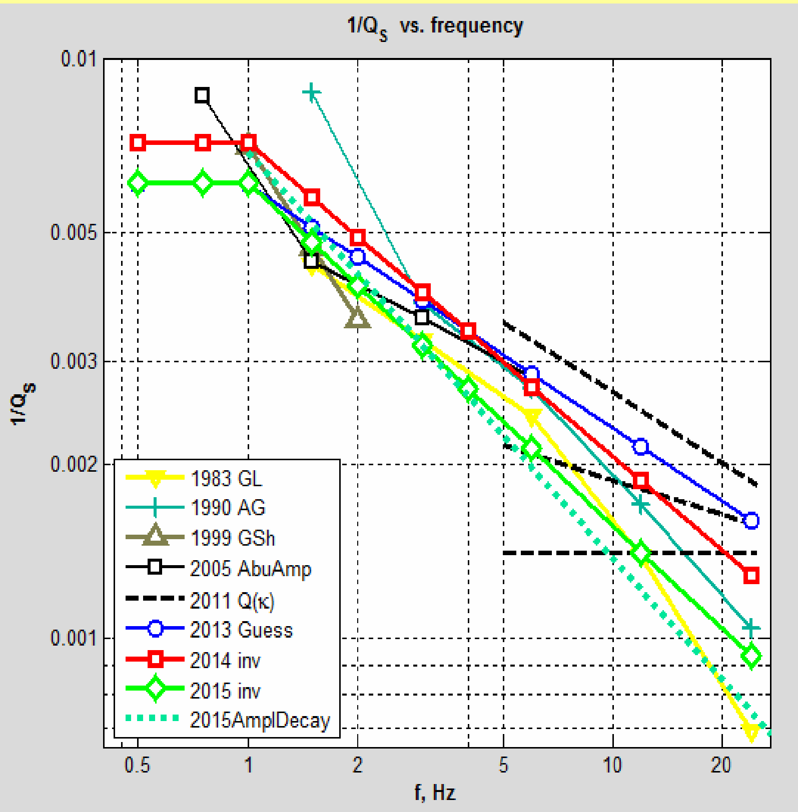

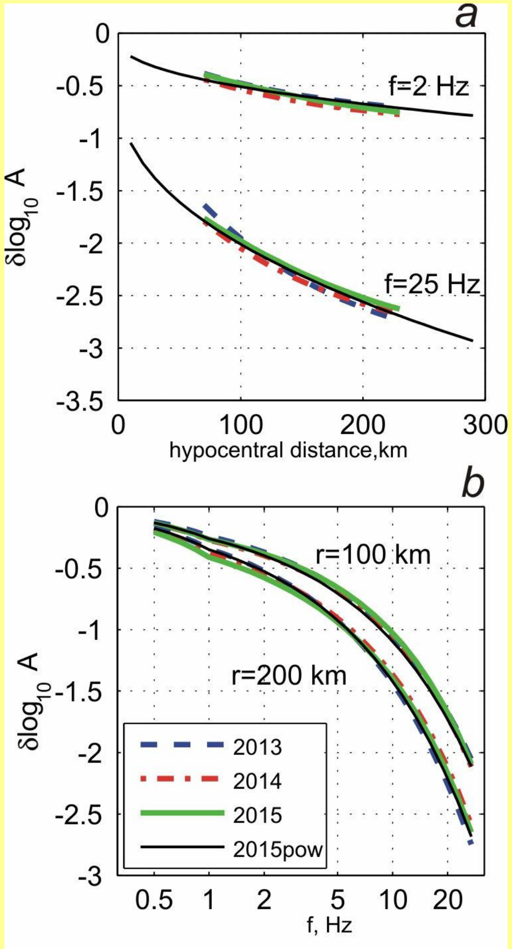

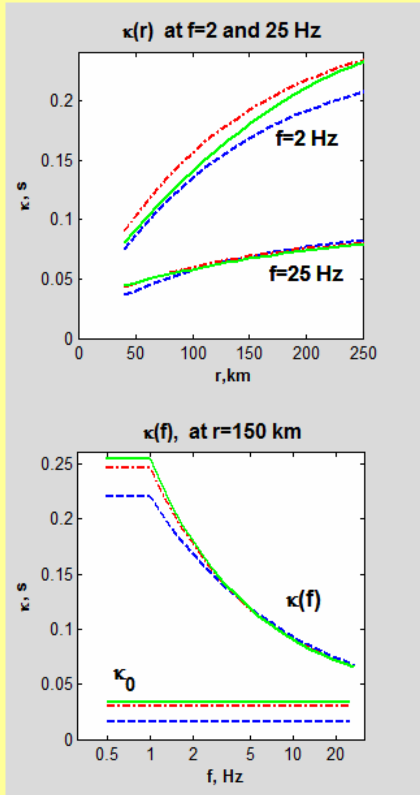

Loss variants **2014** and **2015** match
CONVERGENCE!

$\boldsymbol{f_{c3}(M_0)}$: dlog f_{c3}/dlog M_0 = -0.07±0.011

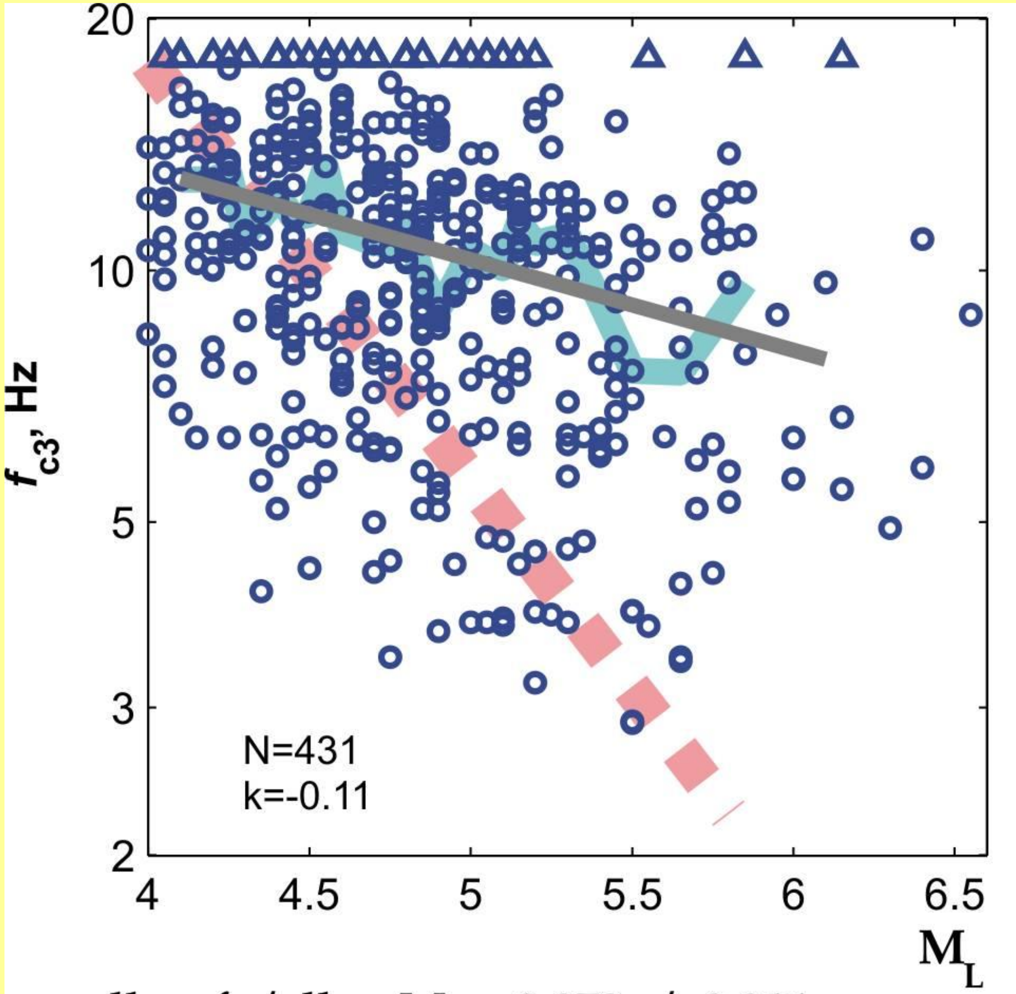

dlog f_{c3} / dlog M_0 = -0.072 +/- 0.011

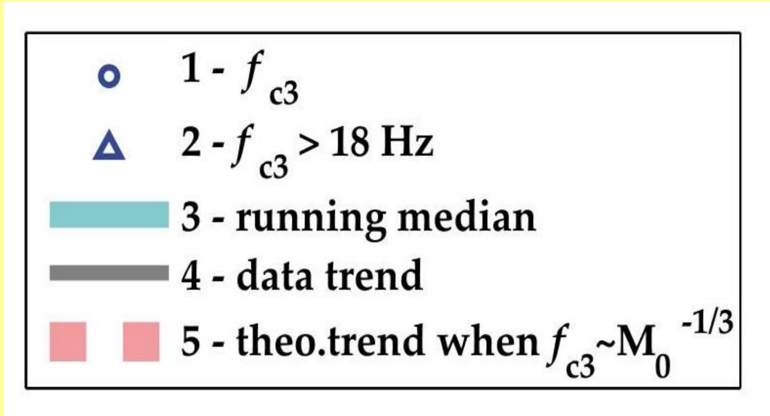

Slope estimates:
-0.07 [2014]
-0.11 [2015, adjusted]

All three trends side by side: see how scaling varies

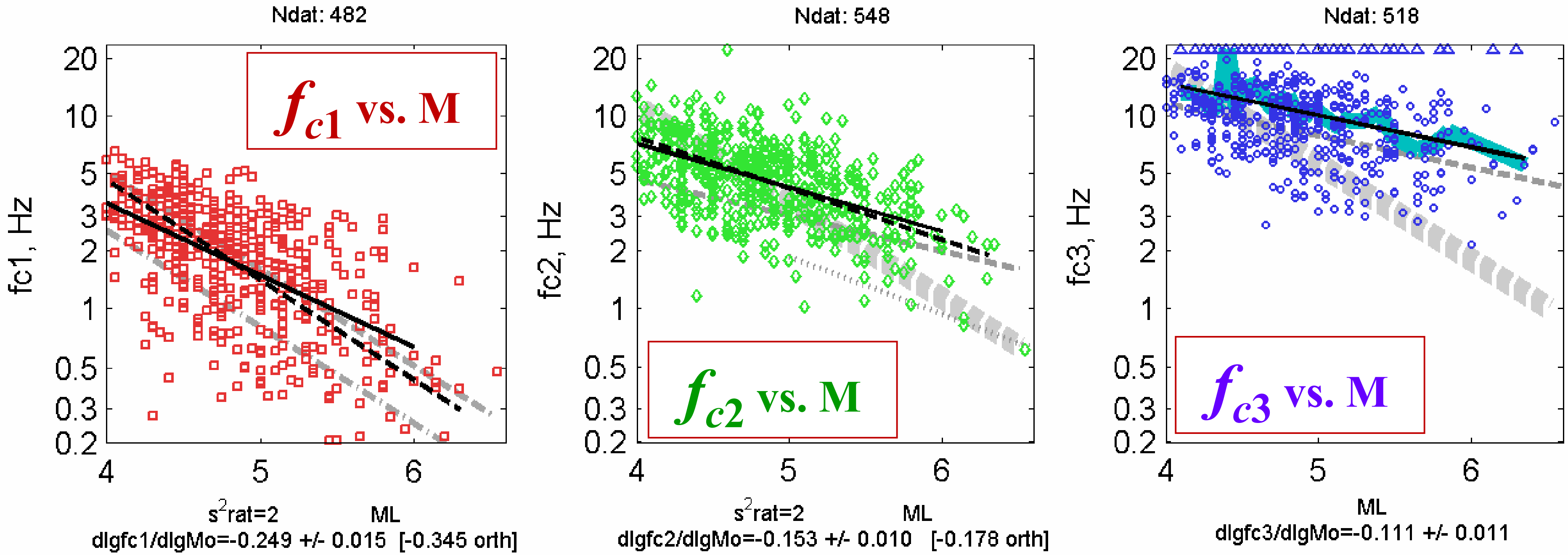

(1) Each of the 3 trends is different

(2) Assumption of *similarity*:

≈holds for f_{c1};

breaks for f_{c2} and f_{c3}

grey trends:
(1) Taiwan, globe
(2) ENA WUSA
(3) Aki 1988

Trend of f_{c3} vs. M_w : new data compared to compilation-2010

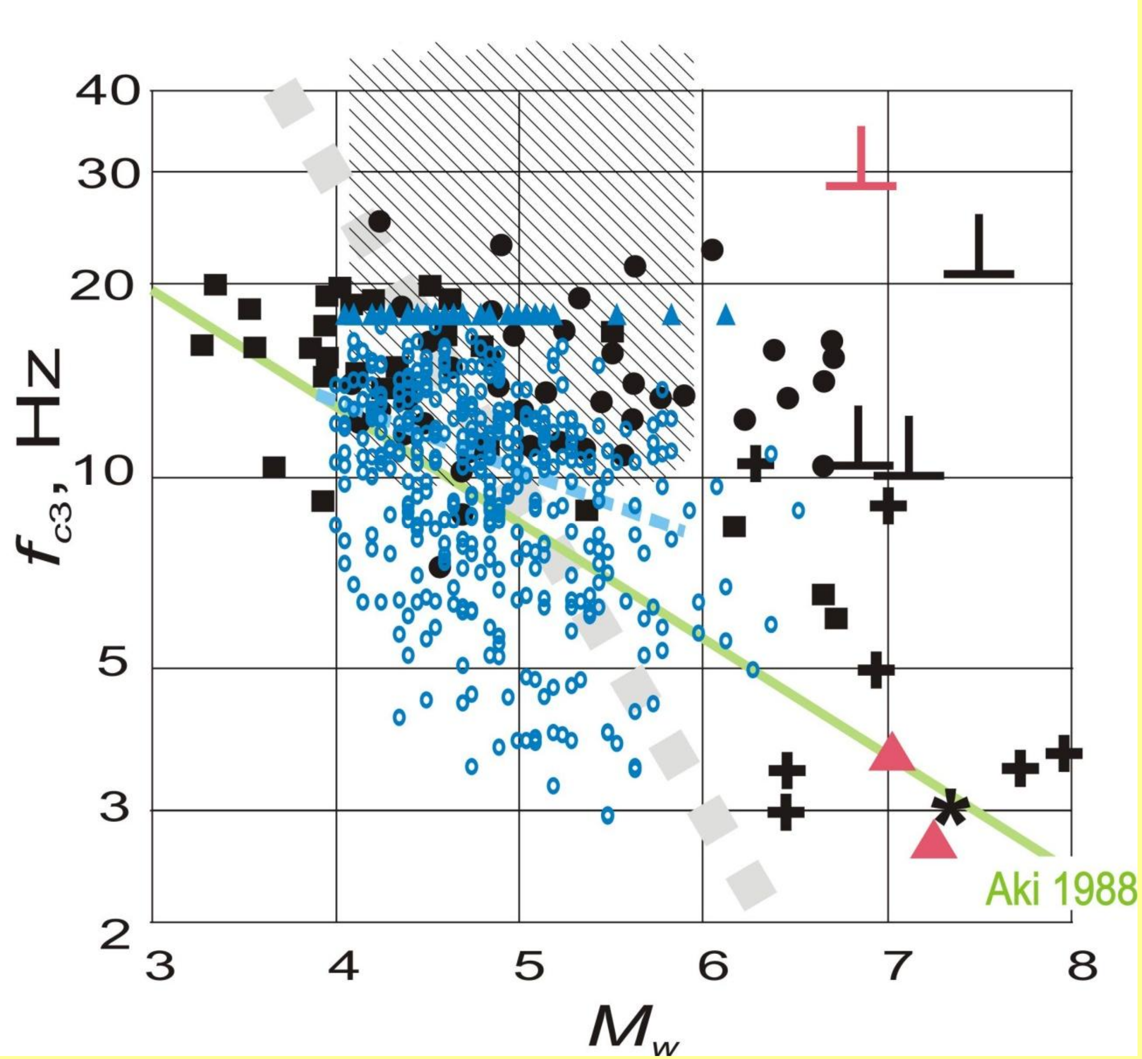

black: compilation [Gusev 2013]

o ▲ 2015 Kamchatka data

Aki 1988

▲⊥ Faccioli 1986

High f_{c3} :

NO ANOMALY

An important part of the general picture

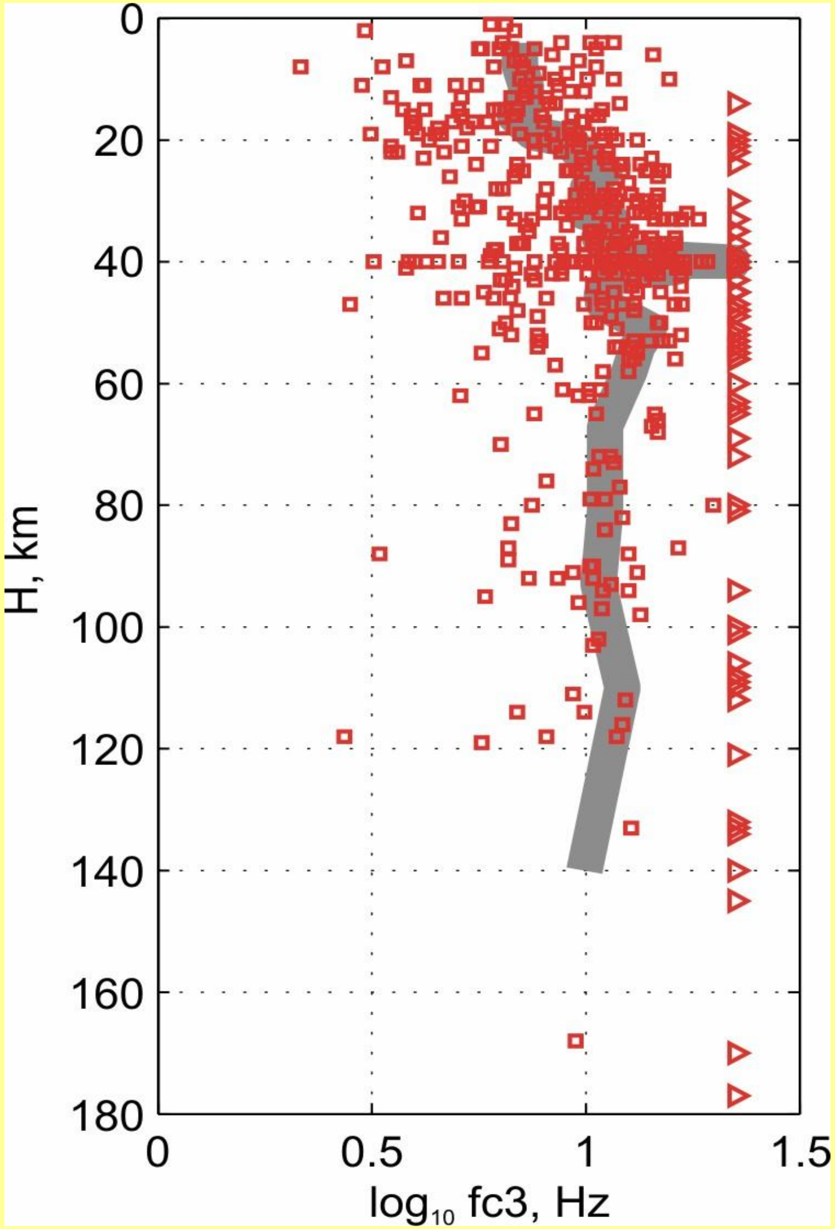

$f_{c3}(H)$

f_{c3} **grows with depth up to 50 km**

Possible physics that underlies the existence of f_{c3} and the trend of f_{c3} vs. M_0

Formation of f_{c3} can be attributed to the summary effect of the following factors:

(1) lower (or high-wavelength) limit of the size of fault surface heterogeneity [Gusev 1990]

(2) finite fault zone thickness (gauge layer etc.)[Papageorgiou&Aki 1983]

(3) finite cohesive zone width [Campillo 1983]

The trend $f_{c3} \propto f_{c1}^{0.2\text{-}0.3}$ or $f_{c3} \propto M_0^{\approx -0.1}$

suggests that f_{c3} slowly decreases with source size

An underlying *cause* of such a trend may be *variations of maturity of fault* surface :

the greater *distance* fault walls have slipped, the larger is their *wear*, and:

(1) the lower is the upper cutoff of heterogeneity spectrum [by abrasion]

(2) the wider/thicker is weak fault zone [by wear product accumulation]

[Gusev 1990; Matsu'ura 1990,1992].

Conclusions

1. Systematic separation of source-controlled and attenuation-controlled constituents of f_{max} is undertaken.
2. To enable this kind of analysis, an attenuation model for the lithosphere around PET station was guessed and then verified in iterative mode using spectral inversion.
3. Among $\approx$500 attenuation-corrected spectra of M=4-6 earthquakes, a large fraction shows source-controlled f_{max}, i.e. the third corner frequency f_{c3}. However, for $\approx$25% spectra, the classical ω^{-2} model is valid.
4. The values of f_{c3} are in the range 3-20 Hz; they slowly decay with magnitude. The distribution of (f_{c3} , M) pairs agrees with earlier work.

thank you for attention

Step 4. $\mathbf{f_{c1}(M)}$: $dlgf_{c1}/dlgM_0 \approx -1/3$

common, regular trend;

in agreement with the similarity concept

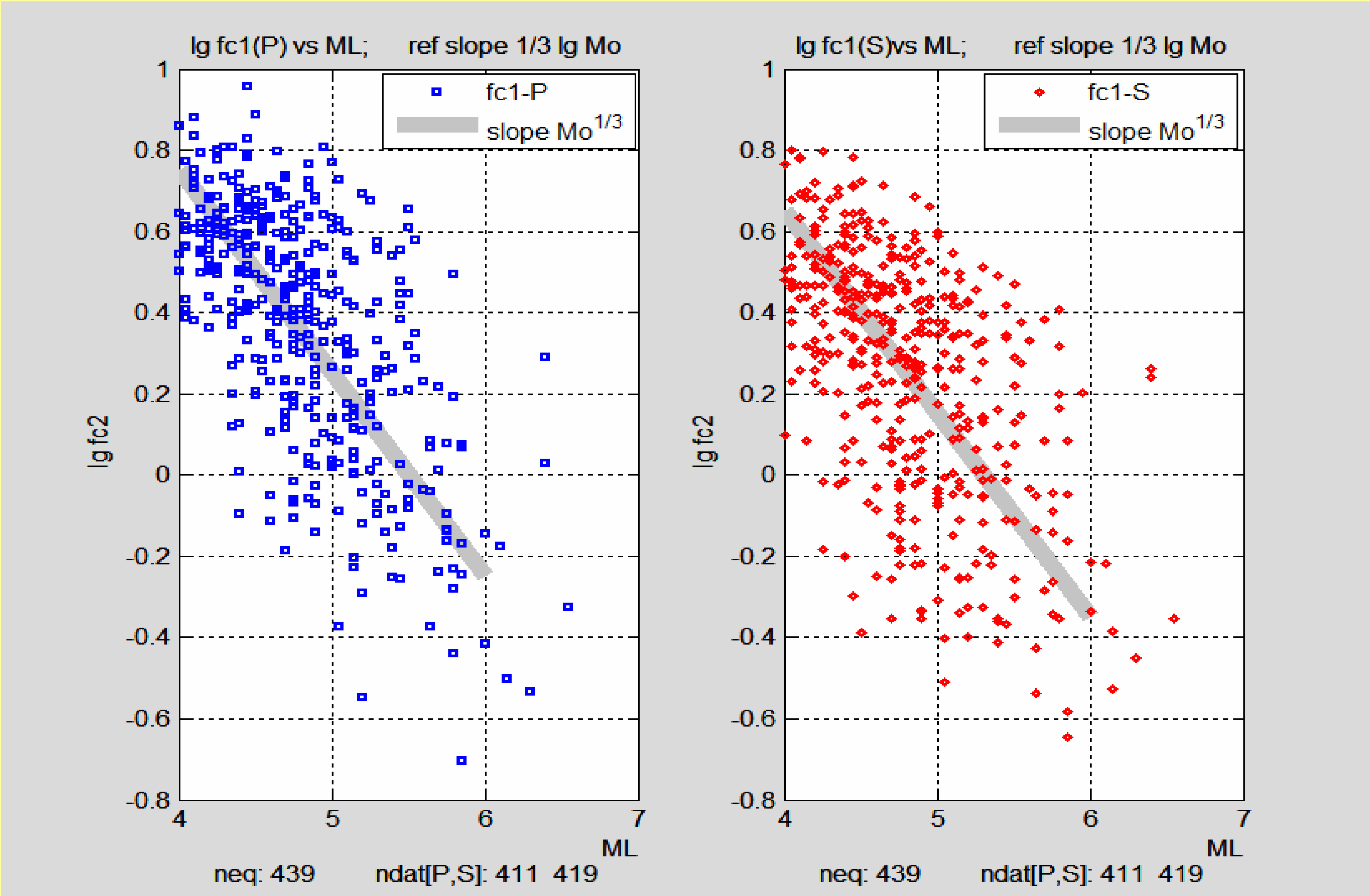

$\mathbf{f_{c2}(M)}$: $dlgf_{c2}/dlgM_0 \approx 0.15\text{-}0.18\ [\pm 0.011] \ll 1/3$

similarity is definitely violated;

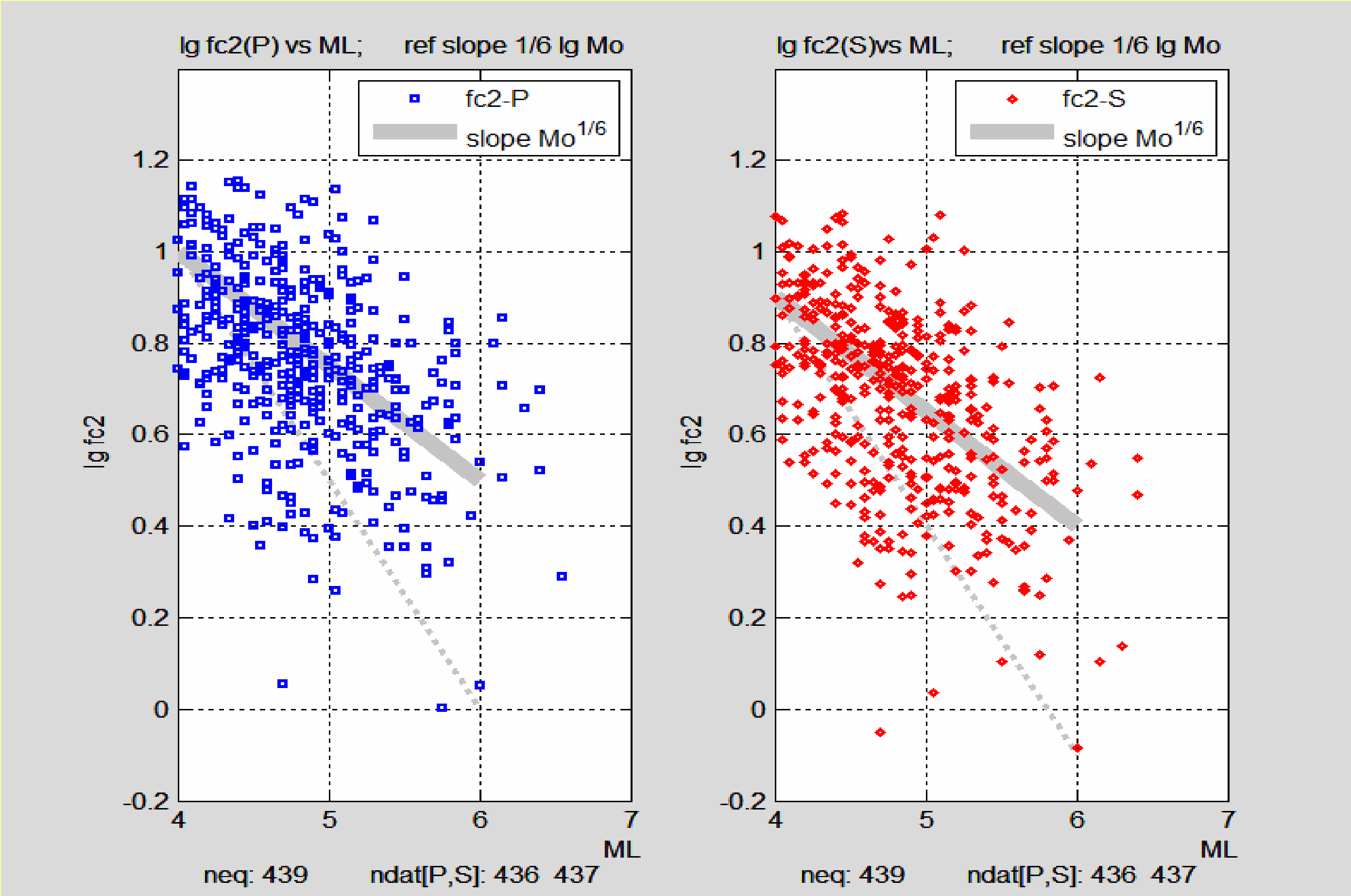

$f_{c3}(M)$: $dlgf_{c1}/dlgM_0 \approx -0.08 \pm 0.013$

no similarity present

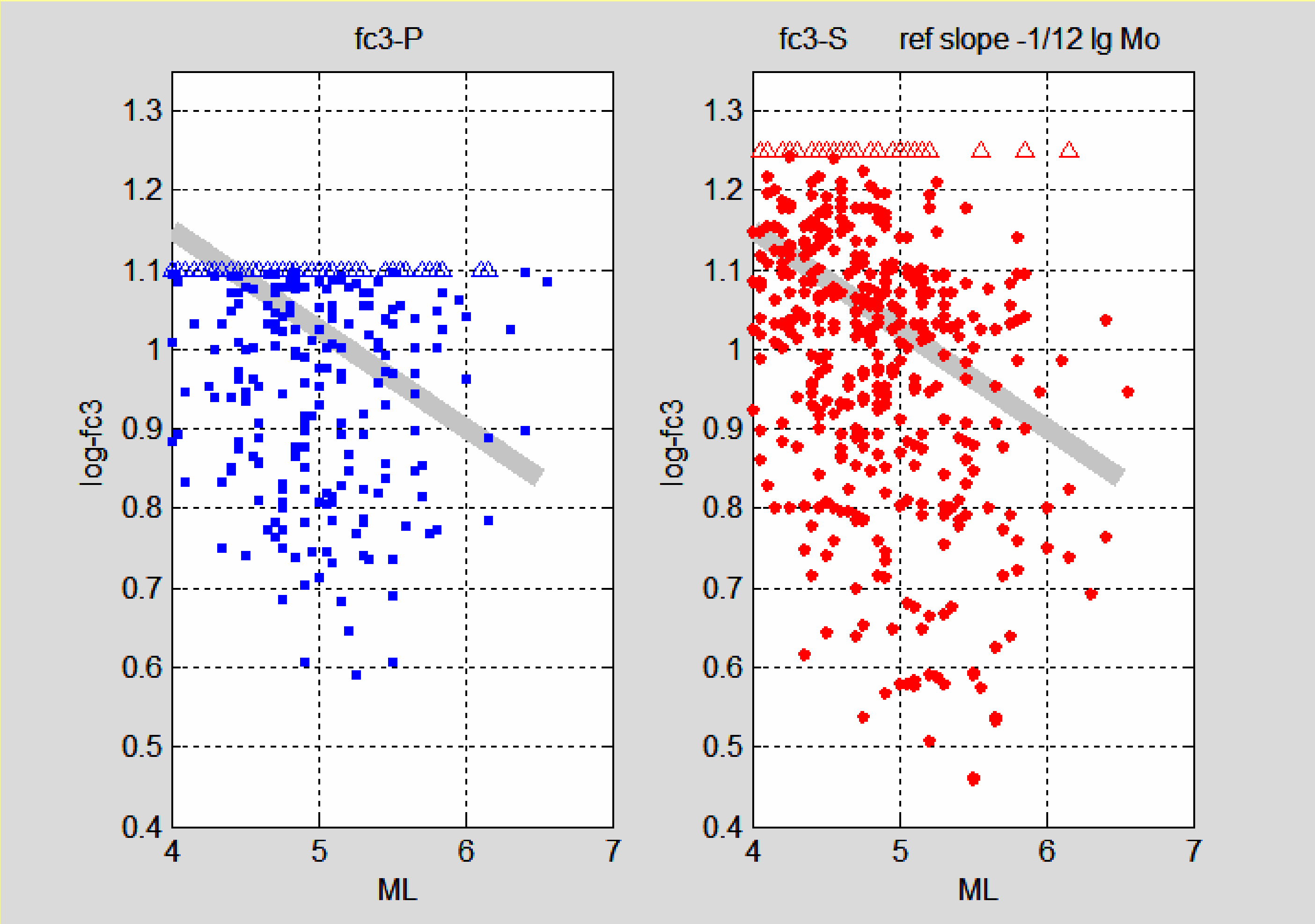

Apparent stress σ_a vs M: no similarity

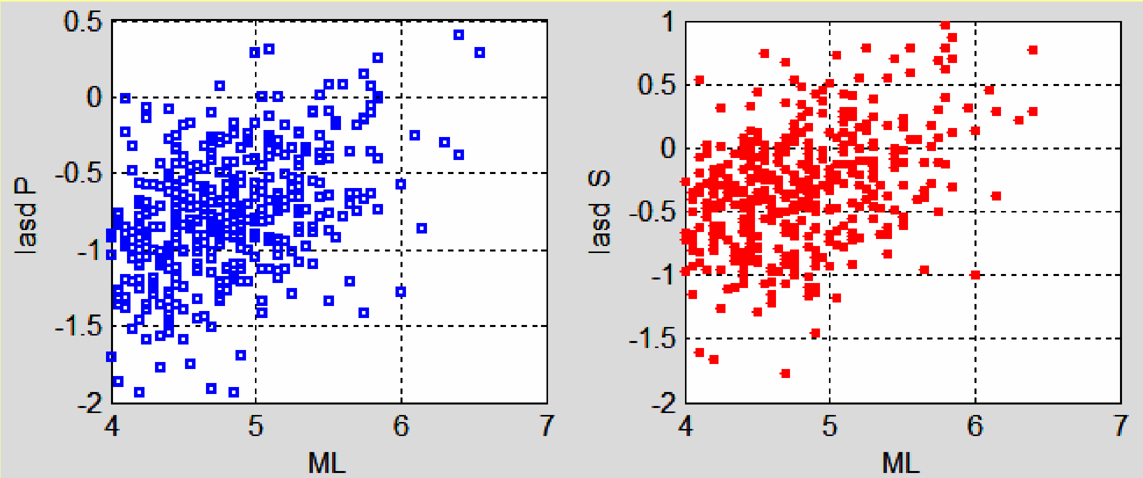

Stress drop $\Delta\sigma$ vs. M: approximate similarity

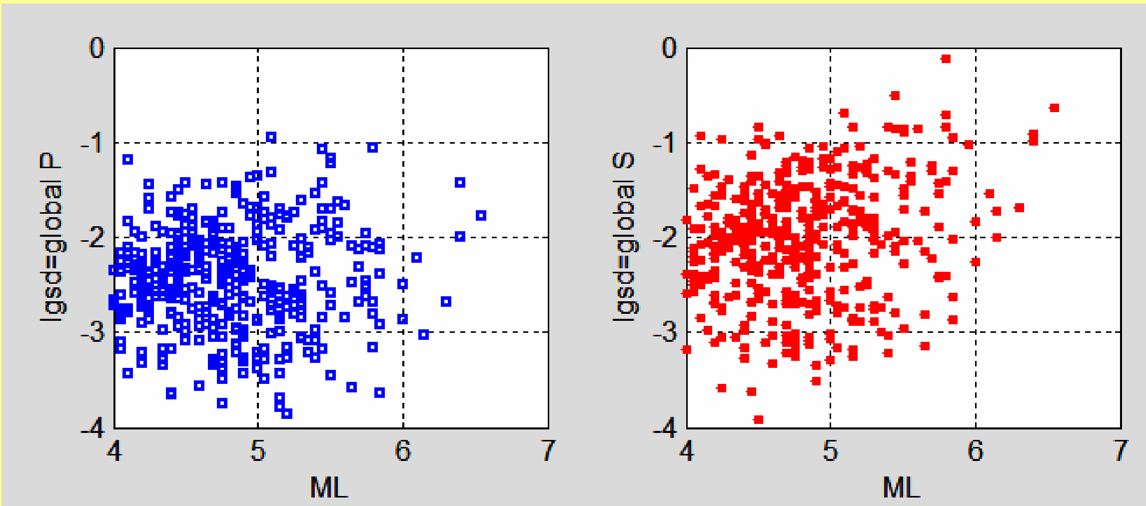

Two ways of checking the similarity assumption make different results

$$\sigma_a = \frac{E_s}{M_0} \propto \frac{v_{\max}^2(f)(f_{c2} - f_{c1})}{d(f)\,|_{f=0}}$$

$$\Delta\sigma \approx \frac{M_0}{R^3} \propto \cdot f_{c1}^3 \cdot d(f)\,|_{f=0}$$

f_{c1} vs. M

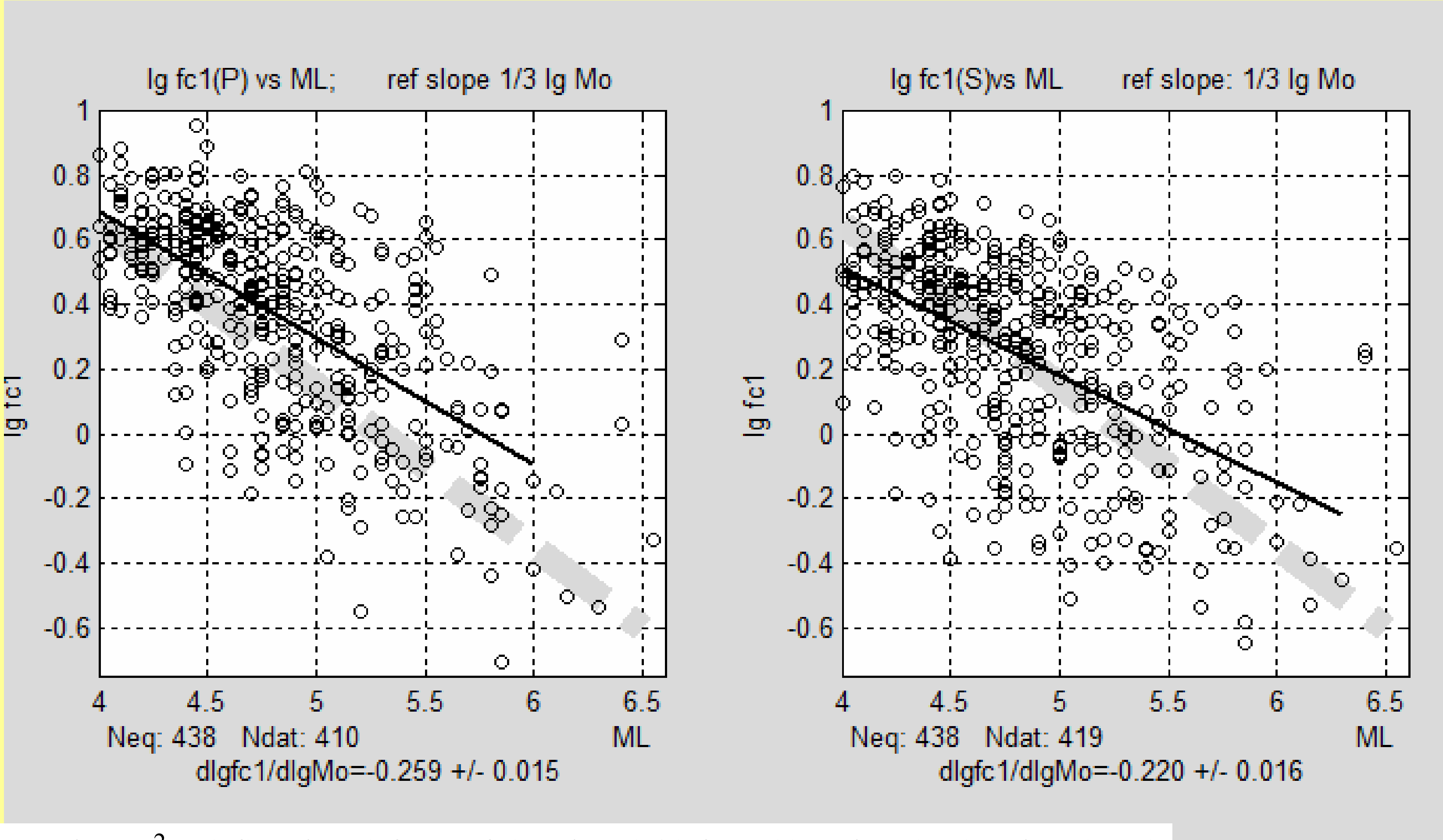

$$\log \sigma_a = \log v_{\max}^2(f) + \log(f_{c2} - f_{c1}) - \log(d(f=0)) = \log(E_s) - \log(M_0)$$

$$\log \Delta\sigma = \log d(f=0) + 3\log(f_{c1}) \quad \text{(all at } r = 1\,\text{km)}$$

$LV = \log f_{c2} - \log f_{c1}$: log-width of velocity spectrum V(f) vs. M
(similarity would result in M-independent LV)

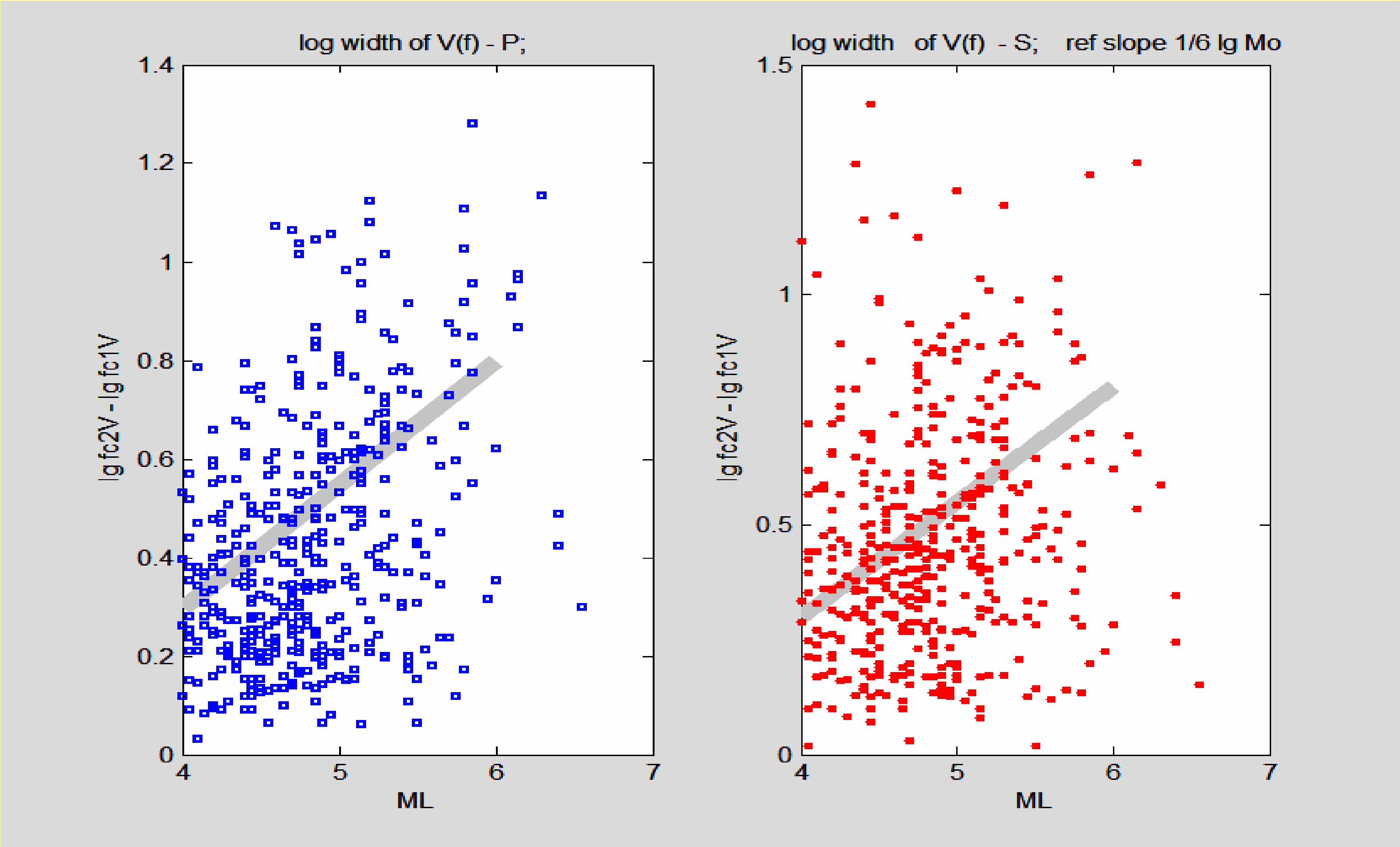

Variation of *LV* with M causes M-dependence of σ_a at a fixed $\Delta\sigma$

Possible physics that underlies trends of f_{c2}, f_{c3}

- **f_{c2}** is probably related to **slip pulse width**;
  the trend $f_{c2} \propto f_{c1}^{0.5\text{-}0.6}$ suggests that pulse width grows by some mechanism akin to random walk

- **f_{c3}** is probably related to the lower limit of the size of fault surface heterogeneity, (or else to cohesion zone width, or both) (compare Aki (1983)), ;
  the trend $f_{c3} \propto f_{c1}^{0.2\text{-}0.3}$ suggests that these parameters increase with source size, however very slowly. Probably this trend reflect variations in fault surface maturity: the greater slipped distance, the larger is accumulated wear and the lower is upper cutoff of heterogeneity spectrum. (compare Gusev 1990; Matsu'ura 1990,1992).